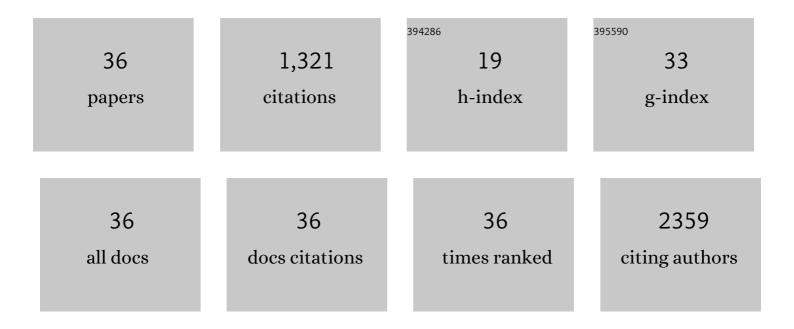
Benedict Law

List of Publications by Year in descending order

Source: https://exaly.com/author-pdf/1280118/publications.pdf Version: 2024-02-01



RENEDICTIAN

#	Article	IF	CITATIONS
1	A Urinary Drug-Disposing Approach as an Alternative to Intravesical Chemotherapy for Treating Nonmuscle Invasive Bladder Cancer. Cancer Research, 2022, 82, 1409-1422.	0.4	Ο
2	Aldoxorubicin-loaded nanofibers are cytotoxic for canine mammary carcinoma and osteosarcoma cell lines in vitro: A short communication. Research in Veterinary Science, 2020, 128, 86-89.	0.9	6
3	Transcriptomic insight into salinomycin mechanisms in breast cancer cell lines: synergistic effects with dasatinib and induction of estrogen receptor β. BMC Cancer, 2020, 20, 661.	1.1	10
4	A combined approach of convection-enhanced delivery of peptide nanofiber reservoir to prolong local DM1 retention for diffuse intrinsic pontine glioma treatment. Neuro-Oncology, 2020, 22, 1495-1504.	0.6	8
5	Multifunctional Nanodelivery Platform for Maximizing Nucleic Acids Combination Therapy. Methods in Molecular Biology, 2020, 2115, 79-90.	0.4	4
6	Real-Time, <i>in Vivo</i> Correlation of Molecular Structure with Drug Distribution in the Brain Striatum Following Convection Enhanced Delivery. ACS Chemical Neuroscience, 2019, 10, 2287-2298.	1.7	25
7	¹⁸ F-Radiolabeled Panobinostat Allows for Positron Emission Tomography Guided Delivery of a Histone Deacetylase Inhibitor. ACS Medicinal Chemistry Letters, 2018, 9, 114-119.	1.3	21
8	Volume of distribution and clearance of peptide-based nanofiber after convection-enhanced delivery. Journal of Neurosurgery, 2018, 129, 10-18.	0.9	12
9	Functional Peptide Nanofibers with Unique Tumor Targeting and Enzymeâ€Induced Local Retention Properties. Advanced Functional Materials, 2018, 28, 1803969.	7.8	32
10	A Murine Model for Quantitative, Real-Time Evaluation of Convection-Enhanced Delivery (RT-CED) Using an 18[F]-Positron Emitting, Fluorescent Derivative of Dasatinib. Molecular Cancer Therapeutics, 2017, 16, 2902-2912.	1.9	15
11	Versatile Nanodelivery Platform to Maximize siRNA Combination Therapy. Macromolecular Bioscience, 2017, 17, 1600294.	2.1	10
12	Chemotherapy induces adaptive drug resistance and metastatic potentials via phenotypic CXCR4-expressing cell state transition in ovarian cancer. PLoS ONE, 2017, 12, e0171044.	1.1	41
13	Smart Nanotransformers with Unique Enzyme-Inducible Structural Changes and Drug Release Properties. Biomacromolecules, 2016, 17, 2040-2049.	2.6	11
14	Longitudinal PET imaging demonstrates biphasic CAR T cell responses in survivors. JCI Insight, 2016, 1, e90064.	2.3	70
15	The receptor for advanced glycation end products influences the expression of its S100 protein ligands in melanoma tumors. International Journal of Biochemistry and Cell Biology, 2014, 57, 54-62.	1.2	18
16	The first characterization of free radicals formed from cellular COX-catalyzed peroxidation. Free Radical Biology and Medicine, 2013, 57, 49-60.	1.3	27
17	A short circulating peptide nanofiber as a carrier for tumoral delivery. Nanomedicine: Nanotechnology, Biology, and Medicine, 2013, 9, 449-457.	1.7	28
18	Cell penetrating peptide tethered bi-ligand liposomes for delivery to brain in vivo: Biodistribution and transfection. Journal of Controlled Release, 2013, 167, 1-10.	4.8	148

Benedict Law

#	Article	IF	CITATIONS
19	Polymeric Nanoparticles with Sequential and Multiple FRET Cascade Mechanisms for Multicolor and Multiplexed Imaging. Small, 2013, 9, 2129-2139.	5.2	59
20	Methods for Conjugating Antibodies to Nanocarriers. Methods in Molecular Biology, 2013, 1045, 249-266.	0.4	8
21	Development of Biocompatible Polymeric Nanoparticles for in Vivo NIR and FRET Imaging. Bioconjugate Chemistry, 2012, 23, 981-992.	1.8	97
22	Novel Synthesis of Stable Polypyrrole Nanospheres Using Ozone. Langmuir, 2011, 27, 13719-13728.	1.6	28
23	Characterization of free radicals formed from COX-catalyzed DGLA peroxidation. Free Radical Biology and Medicine, 2011, 50, 1163-1170.	1.3	20
24	Design and synthesis of a near-infrared fluorescent nanofiber precursor for detecting cell-secreted urokinase activity. Analytical Biochemistry, 2011, 412, 26-33.	1.1	16
25	Relationship between respirometric activity and community of entrapped nitrifying bacteria: Implications for partial nitrification. Enzyme and Microbial Technology, 2010, 46, 229-236.	1.6	59
26	Release of Liposomal Contents by Cell-Secreted Matrix Metalloproteinase-9. Bioconjugate Chemistry, 2009, 20, 1332-1339.	1.8	66
27	Proteolysis: A Biological Process Adapted in Drug Delivery, Therapy, and Imaging. Bioconjugate Chemistry, 2009, 20, 1683-1695.	1.8	115
28	Structural Modification of Protease Inducible Preprogrammed Nanofiber Precursor. Biomacromolecules, 2008, 9, 421-425.	2.6	12
29	Protease-Sensitive Fluorescent Nanofibers. Bioconjugate Chemistry, 2007, 18, 1701-1704.	1.8	48
30	Peptide-Based Biomaterials for Protease-Enhanced Drug Delivery. Biomacromolecules, 2006, 7, 1261-1265.	2.6	90
31	A mitochondrial targeted fusion peptide exhibits remarkable cytotoxicity. Molecular Cancer Therapeutics, 2006, 5, 1944-1949.	1.9	108
32	Optical zymography for specific detection of urokinase plasminogen activator activity in biological samples. Analytical Biochemistry, 2005, 338, 151-158.	1.1	17
33	Mechanism-Based Fluorescent Reporter for Protein Kinase A Detection. ChemBioChem, 2005, 6, 1361-1367.	1.3	10
34	Design, Synthesis, and Characterization of Urokinase Plasminogen-Activator-Sensitive Near-Infrared Reporter. Chemistry and Biology, 2004, 11, 99-106.	6.2	82
35	Tumor Imaging. , 0, , 277-309.		0